

Supporting Information

Baldwin-Type Rules for Metal-Controlled Intramolecular Migratory Insertions. A Computational Study of Ni, Pd and Pt Case.

Béla Fiser,^{a,b,c} Juan M. Cuerva,^{*,d} and Enrique Gómez-BenGoa^{*,a}

^aDepartment of Organic Chemistry I, University of the Basque Country (UPV-EHU), Donostia–San Sebastián, 20018-Spain

^bInstitute of Chemistry, University of Miskolc, Miskolc-Egyetemváros, 3515-Hungary

^cFerenc Rákóczi II. Transcarpathian Hungarian Institute, Beregszász, Transcarpathia, 90200-Ukraine

^dDepartment of Organic Chemistry, University of Granada, Granada, 18071-Spain

INDEX

1. Computational Methods	S2
2. Tables of Results	S3
3. References	S11

Computational Methods

The structures of the study were optimized at DFT level by using the M06¹ functional as implemented in Gaussian 09.² Calculations were carried out by using the 6-31+G(d,p) basis set for C, H and P and Stuttgart/Dresden (SDD) effective core potential (ECP) basis set for Ni, Pd and Pt. Solvent effects were taken into account at the same levels of theory by applying the conductor-like polarizable continuum model (CPCM, Solvent = Dichloromethane). The solute cavity was constructed using radii from the UFF force field. The critical stationary points were characterized by frequency calculations in order to verify that they have the right number of imaginary frequencies, and the intrinsic reaction coordinates (IRC)³ were followed to verify the energy profiles connecting the key transition structures to the correct associated local minima.

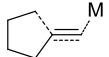
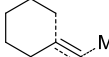
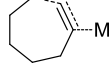
In some cases the transition states were located using M062X/6-31+G(d,p)/SDD level of theory. Thereafter, the resulting structures were used in single point calculations at the M06/6-31+G(d,p)/SDD level of theory. Then, these single point energies were used to get the corresponding Gibbs free energies which are comparable with the ones coming from the above mentioned one step M06/6-31+G(d,p)/SDD calculations.

Table S1. Trig processes: gibbs free activation energies (kcal/mol) computed at the M06/6-311+G(d,p) (PCM,dichloromethane) level for pure anionic cyclizations (none), carbolithiations (Li), carbo-nickelations (Ni), carbo-palladations (Pd) and carbo-platinations (Pt). Values in parenthesis correspond to attacking angles.

		none	Li	Ni	Pd	Pt
	3-exo	13.0 (123)	11.9 (124)	0.5 (112)	2.6 (114)	9.8 (114)
	4-endo	39.3 (77)	53.7 (75)	34.6 (76)	44.3 (76)	52.1 (77)
	4-exo	14.7 (128)	19.6 (127)	16.7 (122)	22.6 (123)	27.5 (123)
	5-endo	16.3 (88)	24.4 (97)	17.5 (89)	26.7 (91)	33.9 (92)
	5-exo	8.7 (122)	10.4 (123)	9.3 (116)	11.9 (119)	18.9 (118)
	6-endo	18.9 (102)	28.2 (109)	8.2 (100)	16.1 (102)	25.5 (103)
	6-exo	13.7 (113)	11.3 (120)	9.8 (120)	15.6 (119)	21.6 (119)
	7-endo	15.4 (110)	21.6 (117)	16.1 (114)	18.4 (115)	26.9 (115)

For comparison, color code corresponds to previous predictions by Baldwin.⁴
 Red: forbidden; Green: Favored. Conflicting predictions are also highlighted.

Table S2. Dig processes: gibbs free activation energies (kcal/mol) computed at the M06/6-311+G(d,p) (PCM,dichloromethane) level for pure anionic cyclizations (none), carbolithiations (Li), carbo-nickelations (Ni), carbo-palladations (Pd) and carbo-platinations (Pt). Values in parenthesis correspond to attacking angles.

		none	Li	Ni	Pd	Pt
	3-exo	18.0 (135)	11.4 (127)	1.0 (126)	3.6 (125)	8.7 (125)
	4-endo	36.4 (77)	41.3 (80)	58.4 (88)	62.9 (86)	64.7 (90)
	4-exo	19.2 (132)	13.1 (127)	9.7 (124)	18.0 (125)	23.7 (125)
	5-endo	14.1 (85)	20.7 (90)	32.5 (103)	40.1 (103)	44.8 (105)
	5-exo	7.5 (124)	9.5 (117)	9.2 (112)	13.2 (116)	20.2 (118)
	6-endo	15.2 (101)	20.5 (107)	12.6 (84)	25.9 (85)	31.8 (85)
	6-exo	12.4 (120)	8.0 (126)	9.6 (106)	21.2 (110)	19.7 (114)
	7-endo	14.9 (116)	18.1 (119)	8.4 (96)	24.2 (103)	21.2 (102)

For comparison, color code corresponds to previous predictions by Alabugin *et al.*⁵ Red: forbidden; Blue: borderline; Green: Favored. Conflicting predictions are highlighted.

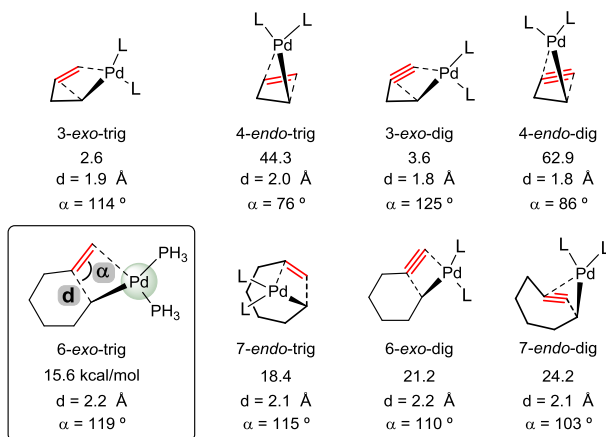
Table S3. Trig processes: reaction Gibbs free energies (in kcal/mol) computed at the M06/6-311+G(d,p) (PCM,dichloromethane) level for pure anionic cyclizations (none), carbolithiations (Li), carbo-nickelations (Ni), carbo-palladations (Pd) and carboplatinations (Pt).

<i>trig</i>	none	Li	Ni	Pd	Pt
3-exo	2.9	0.2	-1.3	3.2	no str.
4-endo	9.2	5.5	6.0	9.0	15.2
4-exo	1.3	2.7	14.3	11.5	22.7
5-endo	-9.7	-7.7	-13.0	-7.3	-0.1
5-exo	-17	-15.8	-7.2	-2.3	2.2
6-endo	-15.4	-13.7	-20.4	-15.6	-6.3
6-exo	-20.2	-22.5	-15.3	-10.7	-5.4
7-endo	-10.2	-10.2	-20.9	-17.8	2.1

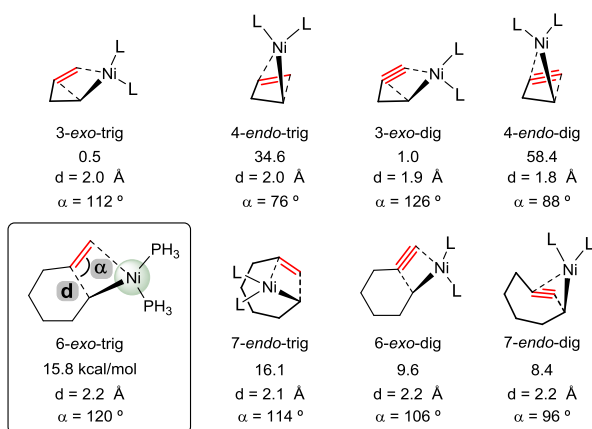
Table S4. Dig processes: reaction Gibbs free energies (in kcal/mol) computed at the M06/6-311+G(d,p) (PCM,dichloromethane) level for pure anionic cyclizations (none), carbolithiations (Li), carbo-nickelations (Ni), carbo-palladations (Pd) and carboplatinations (Pt).

<i>dig</i>	none	Li	Ni	Pd	Pt
3-exo	-5.8	-6.7	0.6	3.5	6.5
4-endo	-8.3	-9.2	6.2	2.7	1.9
4-exo	-14.1	-13.2	1.1	1.0	no str.
5-endo	-31.7	-30.4	-16.5	-16.3	-13.8
5-exo	-34.3	-33.4	-9.9	-19.2	-17.8
6-endo	-34.9	-33.2	-27.5	-22.9	-21.7
6-exo	-34.6	-41	-19.9	-18.7	-13.0
7-endo	-31.9	-30.7	-30.5	-19.8	-28.1

a)



b)



c)

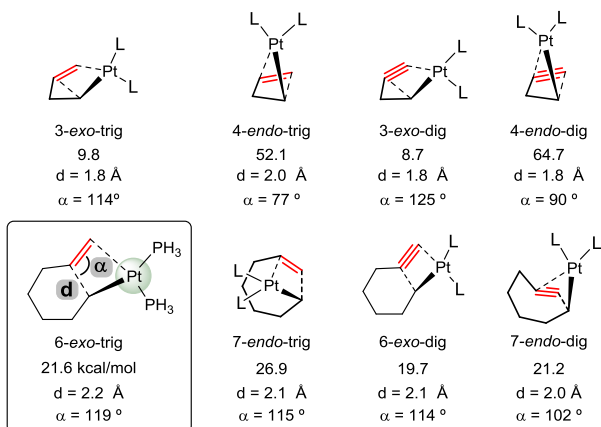


Figure S1. Activation Gibbs Free energies, bond forming distances and attacking angles for border cases (3- and 6-*exo*, 4- and 7-*endo*) in the trig and dig a) carbopalladation, b) carbonickelation and c) carboplatinatation reactions.

Palladium Promoted 3-*exo-trig* Cyclization

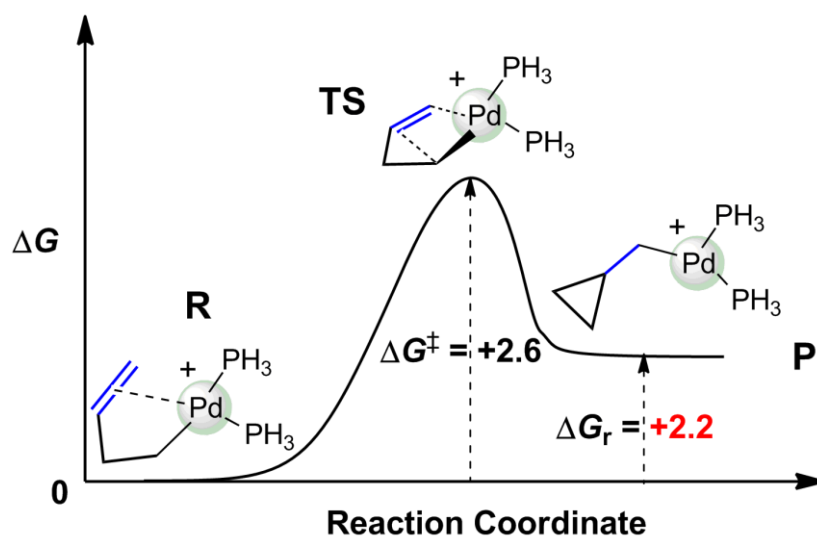


Figure S2. Reaction energy profile of the palladium-promoted 3-*exo-trig* cyclization. ΔG^\ddagger and ΔG_r - activation energy and reaction energy (kcal/mol). R - reactant; TS - transition state; P - product. Calculated at the M06/6-31+G(d,p)/SDD level of theory in dichloromethane.

Scope of the predictions

We decided to study the scope of predictions including structural variations (Figure S3) that could be instructive for a wider understanding of these cyclizations. The 5-*exo* and 6-*endo*-trig carbopalladation pair was selected as the process of reference. For example, similar results were obtained using PMe_3 (II) instead of the unsubstituted PH_3 (I), with a slight reduction of the activation energy only for the *exo* mode (2.1 kcal/mol). These values show that moderate variations in the Tolman's cone angle ($\theta_{\text{PMe}_3}=118^\circ$, $\theta_{\text{PH}_3}=87^\circ$) and electronic properties of the phosphine do not significantly affect the results.

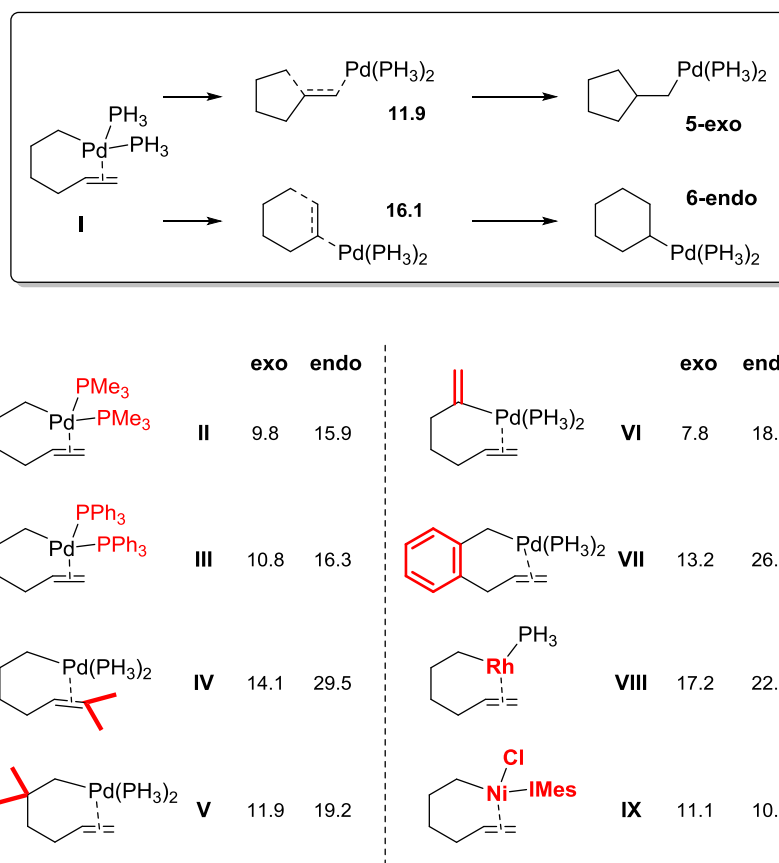


Figure S3. Activation Gibbs Free energies for some computed structural variations of the 5-*exo*-trig and 6-*endo*-trig cyclizations.

If the Palladium center is supported in a sp^2 -carbon (III), which is a very general situation in Heck-type cyclizations, the barrier is fairly reduced in the *exo* case to 7.8 kcal/mol, but slightly increased to 18.7 kcal/mol for *endo*. In this case, sp^2

hybridation of the Carbon somehow reminds of the Baldwin's rules for alkylation of ketone enolates.⁶ The introduction of an aryl moiety within the ring forming chain (**IV**) originates an extra strain and obvious structural difficulties, increasing the barrier in both pathways but especially in the *endo* one (13.2 and 26.0 kcal/mol). More sterically encumbered starting materials, like **V**, where the terminal position of the alkene is occupied by two new methyl groups has a similar effect, increasing the cyclization activation barriers, but again with a significant bias in disfavor of the *endo* mode. We could say that the steric hindrance has a more profound effect on the C-C than on the Pd-C bond formation.

On the other hand, it is usually considered that the introduction of substituents in the tethered chain affects positively cyclization processes through the known Thorpe-Ingold effect,⁷ but in our case, no significant effect was noted in **VI**, where two methyl groups were positioned in one of the Carbon atoms. The energy for the *exo* mode does not vary at all, and a slight increase is just predicted for the *endo* mode. It is worth mentioning that we are measuring the neat cyclization process from the precoordinated alkene-Palladium complex, which can be seen as a cyclic compound by itself. Thus, we are not considering the coordination of the alkene to the metal from the open-chain precursor, which could be the actual source of Thorpe-Ingold rate acceleration. With Rhodium as the metal (**VII**),⁸ the computed activation energies were 17.2 and 22.2 kcal/mol, which are somehow in between those of Palladium (11.9, 16.1 kcal/mol) and Platinum (18.9, 25.5 kcal/mol). Finally, a different coordination pattern was also considered for Nickel complexes (**VIII**), in agreement with the type of ligands used in some experimental cases.^{9,10} A slight increase of ca. 2 kcal/mol was

noted for NHC-type ligands in comparison to its Ni(PH₃)₂, whilst the *exo/endo* energy gap is again very narrow. The two Ni-promoted systems mentioned here (5-*exo* and 6-*endo* for Ni(PH₃)₂ and **VIII**) can be considered as the only examples of our study where the *endo* channel could really compete with the *exo* one.

References

1. Zhao, Y.; Truhlar, D. G. *Theor. Chem. Acc.* 2008, **120**, 215-241.
2. Gaussian 09, Revision D.01; Frisch, M. J.; Trucks, G. W.; Schlegel, H. B.; Scuseria, G. E.; Robb, M. A.; Cheeseman, J. R.; Scalmani, G.; Barone, V.; Mennucci, B.; Petersson, G. A.; Nakatsuji, H.; Caricato, M.; Li, S.; Hratchian, H. P.; Izmaylov, A. F.; Bloino, J.; Zheng, G.; Sonnenberg, J. L.; Hada, M.; Ehara, M.; Toyota, K.; Fukuda, R.; Hasegawa, J.; Ishida, M.; Nakajima, T.; Honda, Y.; Kitao, O.; Nakai, H.; Vreven, T.; Montgomery, J. A. Jr.; Peralta, J. E.; Ogliaro, F.; Bearpark, M.; Heyd, J. J.; Brothers, E.; Kudin, K. N.; Staroverov, V.N.; Keith, T.; Kobayashi, R.; Normand, J.; Raghavachari, K.; Rendell, A.; Burant, J. C.; Iyengar, S. S.; Tomasi, J.; Cossi, M.; Rega, N.; Millam, J. M.; Klene, M.; Knox, J. E.; Cross, J. B.; Bakken, V.; Adamo, C.; Jaramillo, J.; Gomperts, R.; Stratmann, R. E.; Yazyev, O.; Austin, A. J.; Cammi, R.; Pomelli, C.; Ochterski, J. E.; Martin, R. L.; Morokuma, K.; Zakrzewski, V. G.; Voth, G. A.; Salvador, P.; Dannenberg, J. J.; Dapprich, S.; Daniels, A. D.; Farkas, O.; Foresman, J. B.; Ortiz, J. V.; Cioslowski, J.; Fox, J. D. Gaussian, Inc., Wallingford CT, 2013.
3. Gonzalez, C.; Schlegel, H. B. *J. Phys. Chem.* 1990, **94**, 5523–5527.
4. Baldwin, J. E. *J. Chem. Soc., Chem. Commun.* 1976, 734-736.
5. Gilmore, K.; Alabugin, I. V. *Chem. Rev.* **2011**, *111*, 6513-6556.
6. Baldwin, J. E.; Kruse, L. I. *J. Chem. Soc. Chem. Commun.*, 1977, 233.
7. Bachrach, S. M. *J. Org. Chem.* 2008, **73**, 2466.
8. For Rh(III)-catalyzed *exo* cyclizations: Chabaud, L.; Raynal, Q.; Barre, E.; Guillou, C. *Adv. Synth. Cat* 2015, **357**, 3880.
9. Vital, P.; Norrby, P.-O.; Tanner, D. *Synlett* **2006**, *2006*, 3140-3144.
10. Harris, M. R.; Konev, M. O.; Jarvo, E.R. *J. Am. Chem. Soc.* **2015**, *136*, 7825-7828.